Influence of arrangement of layers of composite material on the bearing capacity of a robotic system

Kamil Khayrnasov[1*], *Anton* Sokolskiy[1], and *Vladimir* Isaev[1]

[1]Moscow Aviation Institute (National Research University), 125993 Moscow, Russia

Abstract. The robotic system is considered as a rack made of composite material, which is under dynamic influence. A method for determining the reduced characteristics of a multilayer composite material is given. The simulation of the stand was carried out. To approximate the details of the movement of bench channels: bearings, gearboxes, gear rims, motors, an algorithm and a program for calculating the rigidity of these structures have been developed in order to approximate these elements in the finite element method by replacing such elements with a system of rod structures with rigidity identical to the replaced structures: bearings, gear crowns, gearboxes, motors. The convergence of the calculation results is checked by thickening the finite element mesh. The pinching along the base of the stand was taken as the boundary conditions. A technique has been developed for modeling a three-layer stand structure. The technique for modeling a three-layer structure consists in modeling a stand, assigning filler material to it, and creating shell bearing layers on the surface of the stand, assigning it the characteristics of a multilayer composite material. A layer-by-layer stress-strain state of a stand made of composite material has been obtained. The analysis of the influence of the orientation of the layers of a five-layer composite material on the stress-strain state of the HIL simulation bench has been carried out.

1 Introduction

Robotic systems are widely used in many areas [1-6]. Therefore, the issues of modeling the calculation and analysis of such systems under various operational loads is an important and relevant topic. Robotic systems have bearings, gearboxes, gear rims, motors, the approximation of which is a difficult task, requiring a large amount of theoretical and experimental research in the development and manufacture [7-12]. This study presents an algorithm for calculating the stiffness of such structures and replacing them in the structure with a system of bar structures of identical stiffness. Composite materials are used in many structures, especially in structures where inertial characteristics are of great importance - aircraft building, mechanical engineering [13-20]. In addition, composite materials have a higher specific strength and corrosion resistance compared to homogeneous metals. Since the strength in a multilayer composite material depends of the orientation of the base of the

* Corresponding author: kamilh@mail.ru

layers, it is important to investigate the influence of the location of the layers of the multilayer composite material on the load-bearing capacity of the considered structures of robotic systems: semi-natural simulation stands. When solving such problems, the finite element method is mainly used [21–30].

2 Materials and methods

2.1 Method for determining the reduced characteristics of a multilayer composite material

The plane-stressed state of an orthotropic material was considered, with the coordinate axes coinciding with the axes of the orthotropic of the material. The relationship between stresses and strains was written as

$$\{\sigma\} = [E]\{\varepsilon\}, \tag{1}$$

$$[E] = \begin{Bmatrix} Q_{11} & Q_{12} & 0 \\ Q_{21} & Q_{22} & 0 \\ 0 & 0 & Q_{66} \end{Bmatrix},$$

$\{\varepsilon\}^T = \{\varepsilon_s, \varepsilon_\theta, \varepsilon_{s\theta}\}, \{\sigma\}^T = \{\sigma_s, \sigma_\theta, \sigma_{s\theta}\}$, $Q_{11} = E_s/(1 - v_{s\theta}v_{\theta s})$, $Q_{12} = v_{s\theta}E_s/(1 - v_{s\theta}v_{\theta s})$, $Q_{66} = G_{66}$ $Q_{11} = E_s/(1 - v_{s\theta}v_{\theta s}), Q_{12} = v_{s\theta}E_s/(1 - v_{s\theta}v_{\theta s}), Q_{21} = v_{\theta s}E_s/(1 - v_{s\theta}v_{\theta s}), Q_{22} = E_\theta/(1 - v_{s\theta}v_{\theta s})$,

where $\{\varepsilon\}^T = \{\varepsilon_s, \varepsilon_\theta, \varepsilon_{s\theta}\}$ is deformation vector, $\varepsilon_s, \varepsilon_\theta, \varepsilon_{s\theta}$ is deformations in the direction of the axis s, θ, and in the plane $s\theta$, $\{\sigma\}^T = \{\sigma_s, \sigma_\theta, \sigma_{s\theta}\}$ is the stress vector in the corresponding directions and plane, E_s, E_θ, $v_{s\theta,}v_{\theta s}$ are modulus of elasticity, Poisson coefficients, G_{66} is shear modulus.

When the coordinate axes are rotated through the angle θ, the stress-strain relation matrix can be written as

$$[\bar{E}] = \begin{Bmatrix} \bar{Q}_{11} & \bar{Q}_{12} & \bar{Q}_{16} \\ \bar{Q}_{21} & \bar{Q}_{22} & \bar{Q}_{26} \\ \bar{Q}_{61} & \bar{Q}_{62} & \bar{Q}_{66} \end{Bmatrix}, \tag{2}$$

где $\bar{Q}_{11} = c^4Q_{11} - s^4Q_{22} + 2(Q_{12} + 2Q_{66})s^2c^2, \bar{Q}_{12} = (Q_{11} + Q_{22} - 4Q_{66})s^2c^2 + (s^2+c^2)Q_{22},$

$$\bar{Q}_{16} = (c^2Q_{11} - s^2Q_{12} + (Q_{12} + 2Q_{66})(s^2-c^2))sc, \bar{Q}_{22} = s^4Q_{11} - c^4Q_{22} + 2(Q_{12} + 2Q_{66})s^2c^2, \tag{3}$$

$$\bar{Q}_{26} = (s^2Q_{11} - c^2Q_{12} - (Q_{12} + 2Q_{66})(s^2-c^2))sc, \bar{Q}_{66} = (Q_{11} - 2Q_{12} + Q_{22})s^2c^2 + (s^2-c^2)Q_{66},$$

$$s = \sin\theta\,, c = \cos\theta.$$

When the layer under study is located at a distance z from the middle surface

$$\{\varepsilon\} = \{\varepsilon^o\} + z\{\chi^o\},$$

where $\{\varepsilon^o\}$- deformations of the median surface, $\{\chi^o\}$- deformations of the curvature of the median surface.

Thus, for the stress strain bond, we obtain the dependencies

$$\{\sigma\} = [\bar{Q}]\{\varepsilon^o\} + z[\bar{Q}]\{\chi^o\}. \tag{4}$$

Stresses {σ} can be represented using normal forces N and bending moments M

$$\{N\} = \int_{-h/2}^{h/2}\{\sigma\}dz,\ \{N\}^T = (N_s, N_\theta, N_{s\theta}),\ \{M\} = \int_{-h/2}^{h/2}\{\sigma\}zdz,\ \{M\}^T = (M_s, M_\theta, M_{s\theta}) \quad (5)$$

,

From equation (8) we get

$$\begin{Bmatrix} N \\ M \end{Bmatrix} = [E]\begin{Bmatrix} \varepsilon^o \\ \chi^o \end{Bmatrix},\ [E] = \begin{bmatrix} [A] & [B] \\ [B] & [D] \end{bmatrix} \quad (6)$$

$$[A] = \begin{bmatrix} A_{11} & A_{12} & A_{16} \\ A_{21} & A_{22} & A_{26} \\ A_{61} & A_{62} & A_{66} \end{bmatrix}, [B] = \begin{bmatrix} B_{11} & B_{12} & B_{16} \\ B_{21} & B_{22} & B_{26} \\ B_{61} & B_{62} & B_{66} \end{bmatrix}, [D] = \begin{bmatrix} D_{11} & D_{12} & D_{16} \\ D_{21} & D_{22} & D_{26} \\ D_{61} & D_{62} & D_{66} \end{bmatrix}. \quad (7)$$

$$\{A_{ij}, B_{ij}, D_{ij}\} = \int_{-h/2}^{h/2} Q_{ij}(1, z, z^2)\, dz\,, (i, j = 1,2,3) \quad (8)$$

From equation (8) for a multilayer composite material, we obtain the expression

$$A_{ij} = \sum_{k=1}^{n} \bar{Q}_{ij}(h_k - h_{k-1}), i, j = 1,2,6,\ B_{ij} = \sum_{k=1}^{n} \bar{Q}_{ij}({h^2}_k - {h^2}_{k-1}), i, j = 1,2,6, \quad (9)$$

$$D_{ij} = \sum_{k=1}^{n} \bar{Q}_{ij}({h^3}_k - {h^3}_{k-1}), i, j = 1,2,6,$$

where A_{ij}, B_{ij}, D_{ij} are membrane, flexural-membrane and flexural stiffnesses.

The designations in formulas (9) are shown in Figure 1.

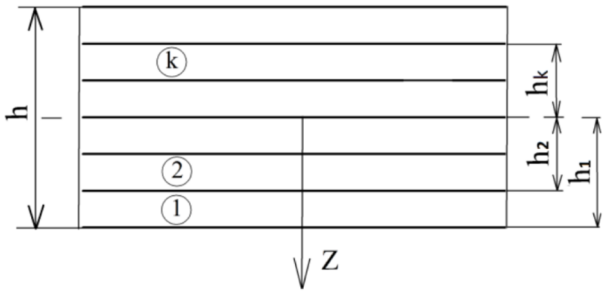

Fig. 1 Multilayer composite structure

2.2 Three-layer composite structure

In the present study, the stand was a three-layer structure, consisting of external carrier layers made of a five-layer composite material with different layer orientations. Inside the carrier layers there was a filler, which is a material of the foam plastic type, which perceives mainly shear stresses and prevents the carrier layers from approaching.

The method of creating a three-layer stand was as follows. A stand was modeled, to which the characteristics of the filler were assigned, then surfaces were created on the model and the characteristics of the carrier layers were assigned to them.

For a three-layer package, transverse shear deformations are taken into account by the shear stiffness matrix.

$$\begin{Bmatrix} \sigma_4 \\ \sigma_5 \end{Bmatrix}^{(k)} = \begin{Bmatrix} \bar{Q}_{44} & 0 \\ 0 & \bar{Q}_{55} \end{Bmatrix}\begin{Bmatrix} \bar{\varepsilon}_4 \\ \bar{\varepsilon}_5 \end{Bmatrix}^{(k)}, \quad (10)$$

where $\bar{Q}_{44} = G_{13}, \bar{Q}_{55} = G_{23}, G_{13}, G_{23}$ are shear moduli.

In the placeholder, the displacements and the angle of rotation are determined from the displacements of the carrier layers.

$$v_2 = (\bar{v}_1 + \bar{v}_3)/2, \quad \varphi_2 = (\bar{v}_1 - \bar{v}_3)/t, \quad \bar{v}_1 = v_1 - t_1 e_{13}/2, \quad \bar{v}_3 = v_3 + t_3 e_{23}/2, \tag{11}$$

where t is the thickness of the three-layer package, t_1 and t_2 are the thicknesses of the carrier layers, t_3 is the thickness of the filler, e_{13},e_{23} are the deformations of the carrier layers, v_3 is the displacement of the neutral axis of the filler, and $\bar{v}_1, \bar{v}_3$ are the displacements of the carrier layers. Moving and the angle of rotation of the filler normal are determined from the relations

$$v_2(z) = v_1 + z\varphi_2 = 0.5(v_1 - t_1 e_{13}/2 + v_3 + t_3 e_{23}/2) + z(v_1 - t_1 e_{13}/2 - v_3 - t_3 e_{23}/2)/t_2,$$
$$u_2(z) = u_1 + z\varphi_2 = 0.5(u_1 - t_1 e_{13}/2 + u_3 + t_3 e_{23}/2) + z(u - t_1 e_{13}/2 - u_3 - t_3 e_{23}/2)/t_2, \tag{12}$$
$$w_2(z) = w_2 + z(w_3 - w_1)/t_2.$$

The ratios can be applied to an arbitrary number of layers. When considering a three-layer package, displacements are taken according to the law of a broken line.

2.3 Method for determining the rigidity of gearboxes, bearings and gear rims.

In this paper, the identification of such elements of robotic systems as bearings, gear rims and gearboxes is carried out in the finite element method by determining the rigidity characteristics of these elements and replacing them in the model with rod systems in terms of stiffness corresponding to the stiffness of the replaced bearings, gear rims and gearboxes. Since the direct modeling of these elements leads to an unjustified increase in the resolving equations and does not perform the functions of these elements in the model. The developed program for determining the stiffness of the elements under consideration takes into account the moments of inertia, angular accelerations and speeds, as well as gear ratios, stiffness and natural frequency of gearboxes and bearings. When calculating the reducer, it is necessary to calculate the equivalent diameter. The developed method and program for determining the stiffness and natural frequency of the gearbox makes it possible to calculate these characteristics for an arbitrary section of the gearbox shafts. The equivalent diameter allows you to determine the stiffness of the gearbox as a whole, the stiffness and frequency.

Calculated according to the developed program, the rigidity of gearboxes, bearing supports and gear rims makes it possible to replace these elements with a rod system identical in rigidity to the part under consideration. The results obtained were compared with the available experimental data, which confirmed the validity of such a replacement. When assigning characteristics to the bearing layers of the stand, it is necessary to position the base of the material at an angle of zero degrees to the trajectories of maximum stresses. Such trajectories can be obtained and corrected according to the results of the calculation of the stand from a homogeneous and composite material. The arrangement of the base of the multilayer composite material along the trajectories of maximum stresses makes it possible to achieve maximum rigidity of the structure, which contributes to the accuracy of positioning of the bench channels, which affect the accuracy of the results obtained and are one of the main characteristics of such structures. The considered technique of modeling, approximation is applicable to most robotic structures.

3 Calculation results

The stand the displacement of the original object in three degrees of freedom and is designed to simulate flight characteristics in laboratory conditions. This allows you to significantly save funding for aircraft testing. The design of the stand (Figure 2) consists of a base, connected by means of a toothed rim with a course fork. In the stand of the course

fork, on the bearings of the supports, there is a pitch ring, inside of which there is a roll channel. Rigid pinching of the stand base is used as boundary conditions.

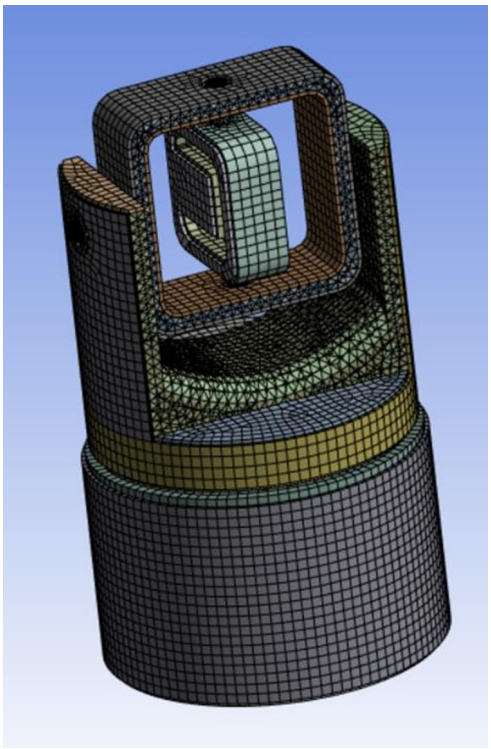

Fig. 2. Bench model approximated by finite elements

The stand is approximated by finite elements (Figure 2), while bearings, gear rims, gearboxes are replaced by a system of rod elements of identical rigidity. The convergence of the results of the finite element approximation was checked by comparing the results when splitting into 3210014 and 425020 finite elements. The discrepancy between the results for such approximations was no more than 3%. The calculation of the stress-strain state of the stand for dynamic acceleration around the vertical axis of the course channel is carried out. Figure 3 shows the layer-by-layer stress-strain state of a five-layer composite material with layer orientation a) 0°/45°/90°/-45°/0° and b) with layer orientation 0°/45°/0°/-45°/0°.

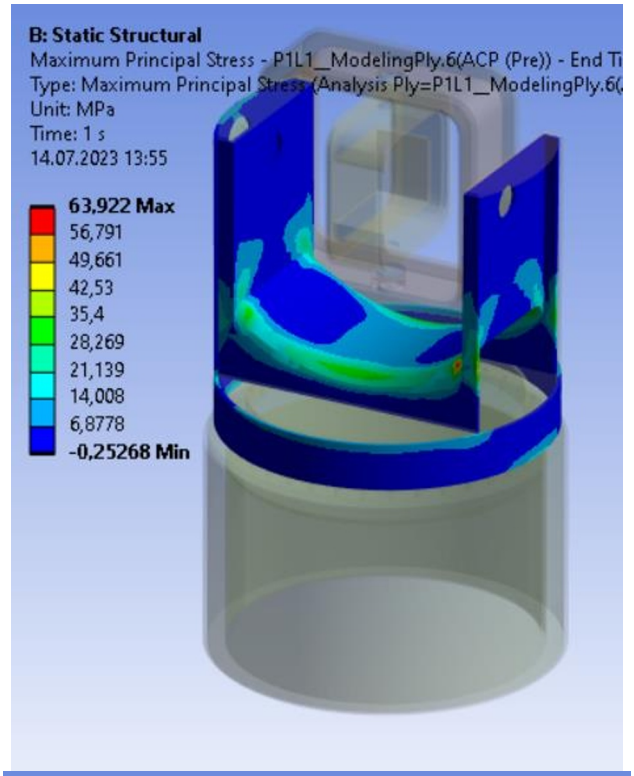
B: Static Structural
Maximum Principal Stress - P1L1_ModelingPly.6(ACP (Pre)) - End Ti
Type: Maximum Principal Stress (Analysis Ply=P1L1_ModelingPly.6(
Unit: MPa
Time: 1 s
14.07.2023 13:55
63,922 Max
56,791
49,661
42,53
35,4
28,269
21,139
14,008
6,8778
-0,25268 Min

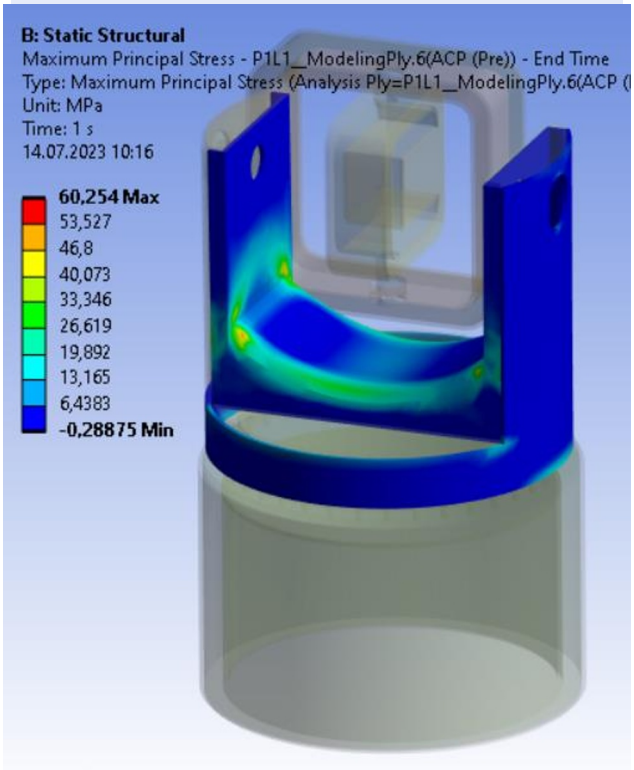
B: Static Structural
Maximum Principal Stress - P1L1_ModelingPly.6(ACP (Pre)) - End Time
Type: Maximum Principal Stress (Analysis Ply=P1L1_ModelingPly.6(ACP (
Unit: MPa
Time: 1 s
14.07.2023 10:16
60,254 Max
53,527
46,8
40,073
33,346
26,619
19,892
13,165
6,4383
-0,28875 Min

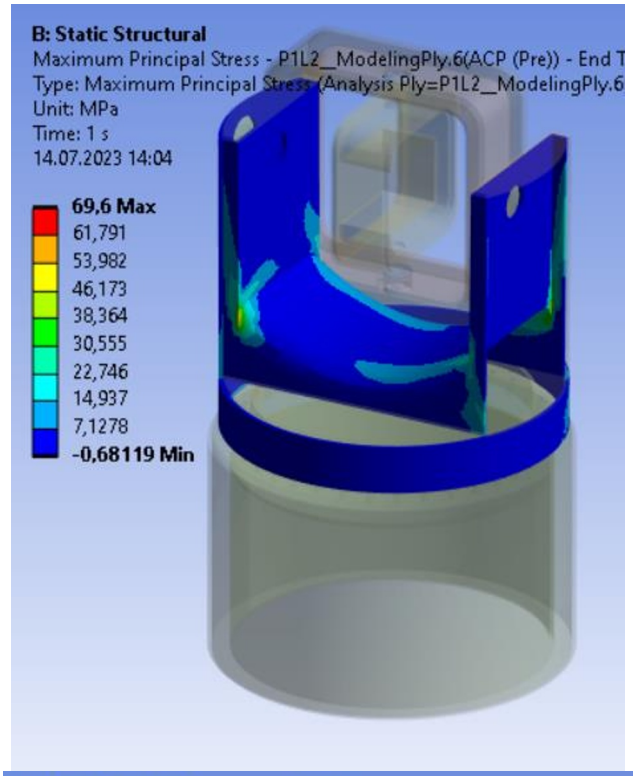
B: Static Structural
Maximum Principal Stress - P1L2__ModelingPly.6(ACP (Pre)) - End T
Type: Maximum Principal Stress (Analysis Ply=P1L2__ModelingPly.6
Unit: MPa
Time: 1 s
14.07.2023 14:04
69,6 Max
61,791
53,982
46,173
38,364
30,555
22,746
14,937
7,1278
-0,68119 Min

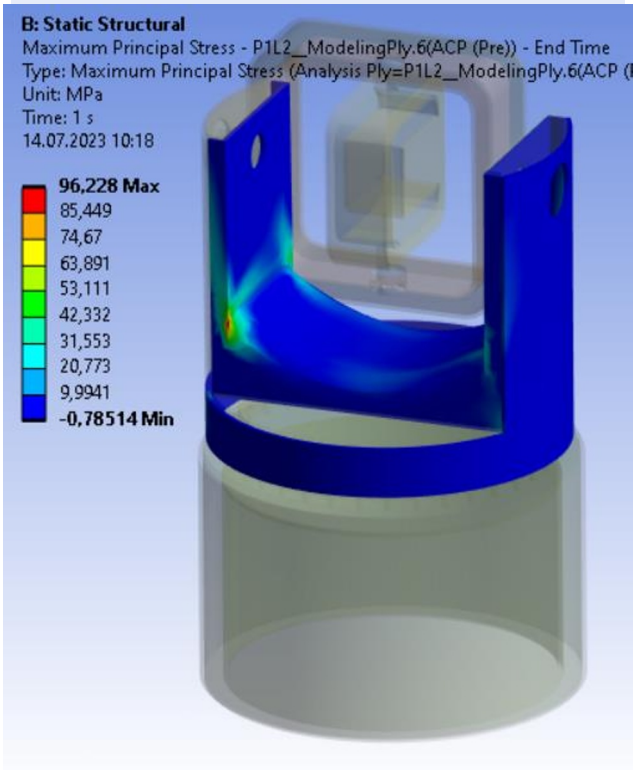
B: Static Structural
Maximum Principal Stress - P1L2__ModelingPly.6(ACP (Pre)) - End Time
Type: Maximum Principal Stress (Analysis Ply=P1L2__ModelingPly.6(ACP (
Unit: MPa
Time: 1 s
14.07.2023 10:18
96,228 Max
85,449
74,67
63,891
53,111
42,332
31,553
20,773
9,9941
-0,78514 Min

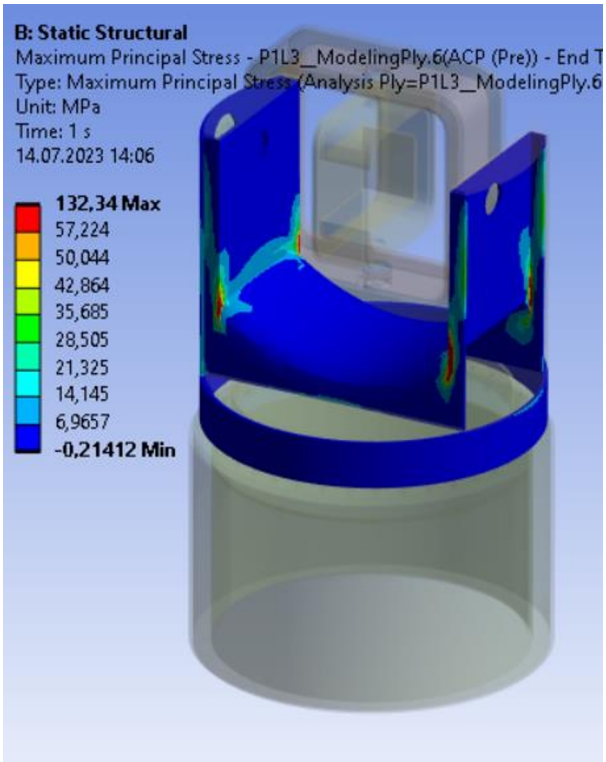
B: Static Structural
Maximum Principal Stress - P1L3_ModelingPly.6(ACP (Pre)) - End T
Type: Maximum Principal Stress (Analysis Ply=P1L3_ModelingPly.6
Unit: MPa
Time: 1 s
14.07.2023 14:06
132,34 Max
57,224
50,044
42,864
35,685
28,505
21,325
14,145
6,9657
-0,21412 Min

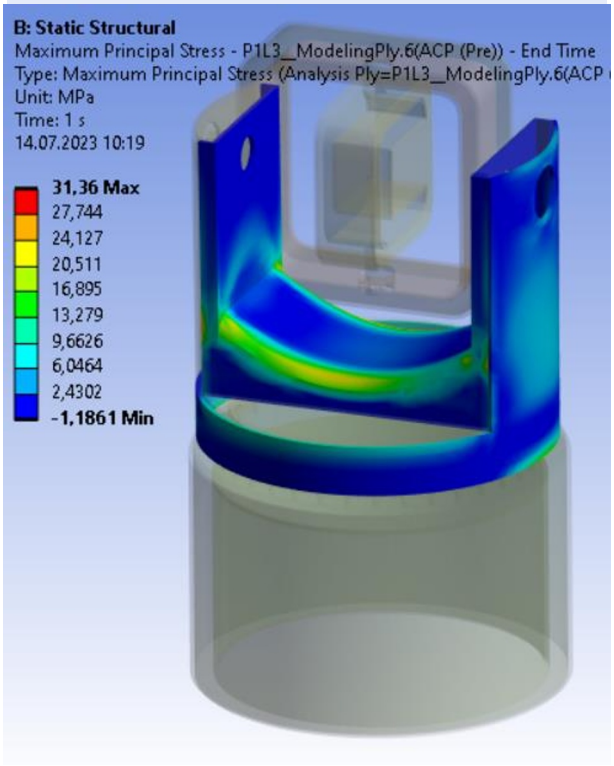
B: Static Structural
Maximum Principal Stress - P1L3_ModelingPly.6(ACP (Pre)) - End Time
Type: Maximum Principal Stress (Analysis Ply=P1L3_ModelingPly.6(ACP
Unit: MPa
Time: 1 s
14.07.2023 10:19
31,36 Max
27,744
24,127
20,511
16,895
13,279
9,6626
6,0464
2,4302
-1,1861 Min

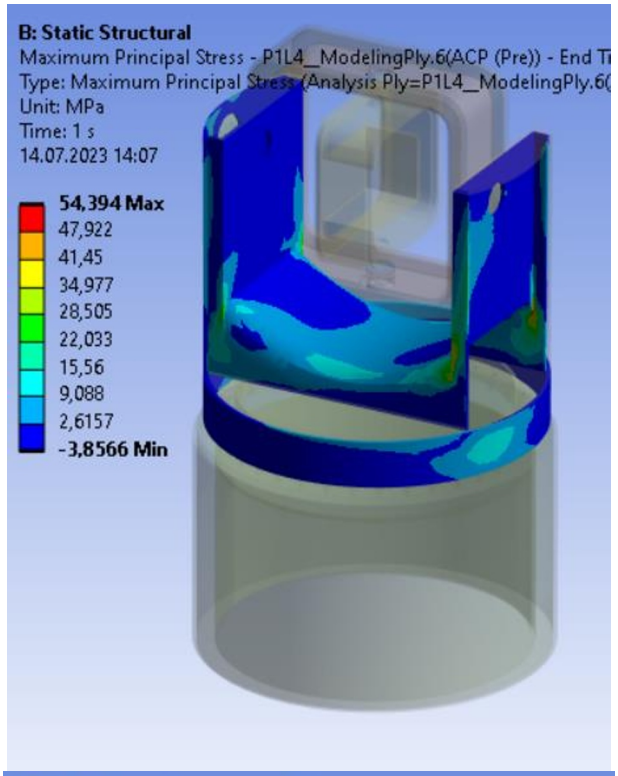
B: Static Structural
Maximum Principal Stress - P1L4_ModelingPly.6(ACP (Pre)) - End Ti
Type: Maximum Principal Stress (Analysis Ply=P1L4_ModelingPly.6(
Unit: MPa
Time: 1 s
14.07.2023 14:07
54,394 Max
47,922
41,45
34,977
28,505
22,033
15,56
9,088
2,6157
-3,8566 Min

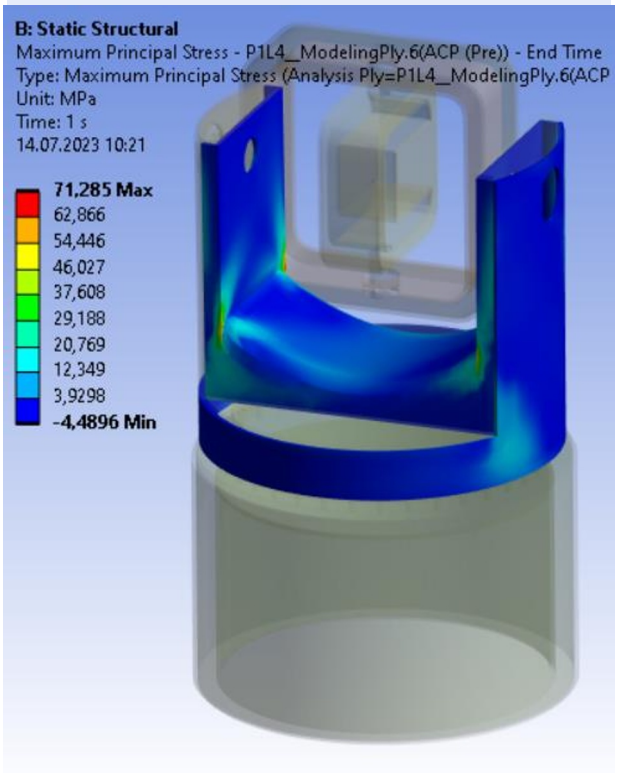
B: Static Structural
Maximum Principal Stress - P1L4_ModelingPly.6(ACP (Pre)) - End Time
Type: Maximum Principal Stress (Analysis Ply=P1L4_ModelingPly.6(ACP
Unit: MPa
Time: 1 s
14.07.2023 10:21
71,285 Max
62,866
54,446
46,027
37,608
29,188
20,769
12,349
3,9298
-4,4896 Min

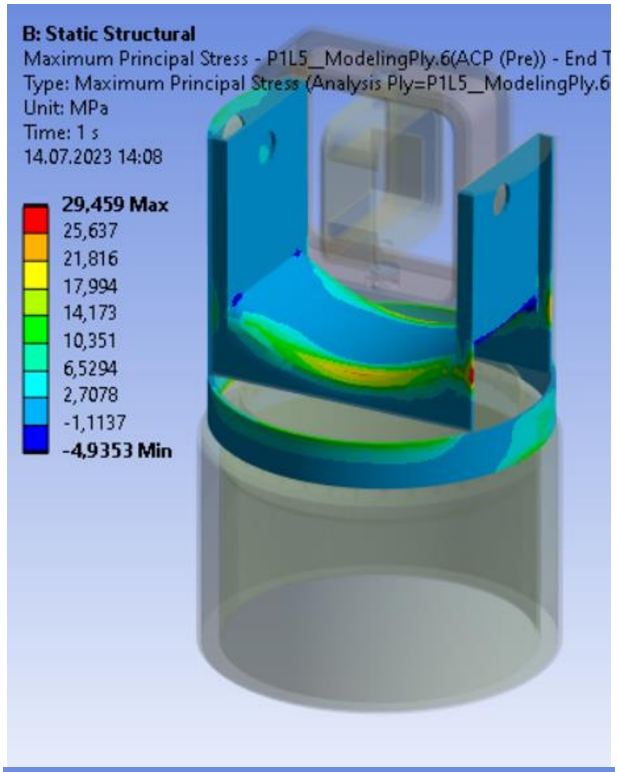
B: Static Structural
Maximum Principal Stress - P1L5__ModelingPly.6(ACP (Pre)) - End T
Type: Maximum Principal Stress (Analysis Ply=P1L5__ModelingPly.6
Unit: MPa
Time: 1 s
14.07.2023 14:08
29,459 Max
25,637
21,816
17,994
14,173
10,351
6,5294
2,7078
-1,1137
-4,9353 Min

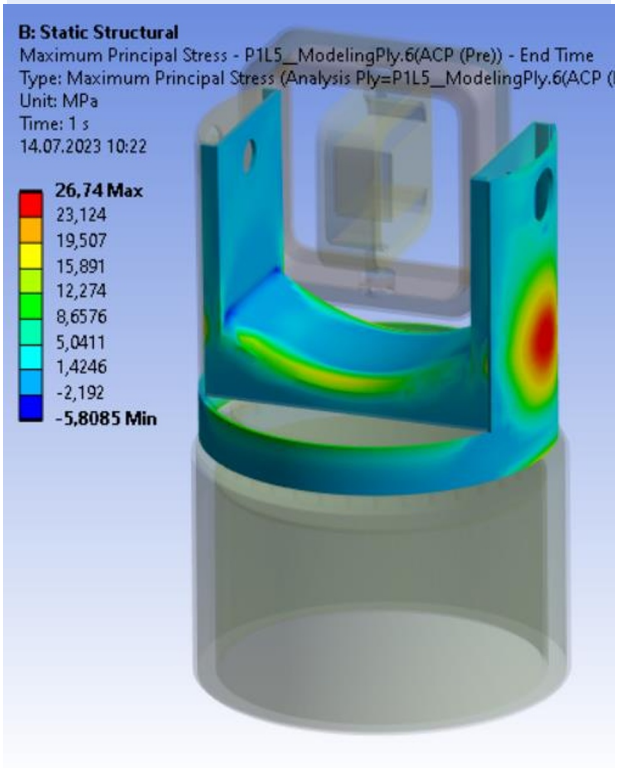
B: Static Structural
Maximum Principal Stress - P1L5__ModelingPly.6(ACP (Pre)) - End Time
Type: Maximum Principal Stress (Analysis Ply=P1L5__ModelingPly.6(ACP (
Unit: MPa
Time: 1 s
14.07.2023 10:22
26,74 Max
23,124
19,507
15,891
12,274
8,6576
5,0411
1,4246
-2,192
-5,8085 Min

Fig, 3. Stresses by layers in a five-layer composite material: a) layer orientation 0º/45º/0º/-45º/0º and b) layer orientation 0º/45º/90º/-45º/0º under dynamic loading of the heading channel with an angular velocity of 500 rad/ with around the vertical axis of the stand

As can be seen from Figure 3, the highest stress is observed in the third layer of 136 MPa, where the layer orientation is perpendicular to the trajectory of maximum stresses.

Calculations were also carried out for a stand made of a composite material with the orientation of the layers 0º/75º/0º/-75º/0º, 0º/15º/90º/-15º/0º and 0º/0º/90º/90º/0º. The calculation results are summarized in Table 1.

Table 1 shows the maximum stresses in the layers of a five-layer composite material depending on the orientation of the layers. 1 layer is located on the surface of the model. An analysis of the obtained stresses of the bench at dynamic angular velocity showed that the most favorable arrangement of the orientation of the layers on the stress state of the structure under study corresponds to the first line of Table 1

Table 1. Influence of the orientation of the layers in a five-layer composite material on the maximum values of the stresses of the layers. Layer orientation st layer 1st layer, MPa, 2nd layer, MPa, 3rd layer, MPa, 4th layer, MPa, 5th layer, MPa.

Layer orientation	1st layer, MPa	2st layer, MPa	3st layer, MPa	4st layer, MPa	5st layer, MPa
0º/45º/0º/-45º/0º	60,25	96,23	31,36	71,29	26,74
0º/45º/90º/-45º/0º	63,92	64,60	132,34	54,39	29,46
0º/75º/0º/-75º/0º	60,43	117,23	57,23	92,58	21,88
0º/15º/90º/-15º/0º	57,28	39,35	135,94	26,05	21,64
0º/0º/90º/90º/0º	55,52	38,87	103,84	85,44	23,08

As can be seen from the table 1, the five-layer composite material in the stand under dynamic loading is the most durable, consisting of the orientation of the layers 0º/45º/0º/-45º/0º and 0º/0º/90º/90º/0º and the weakest when the layers are oriented 0º/15º/90º/-15º/0º, 0º/45º/90º/-45º/0º. Zero orientation corresponds to the direction of the trajectory of maximum stresses.

4 Conclusions

As a result of the study, modeling and approximation by finite elements of the semi-natural simulation stand were performed. The calculation of the stress-strain state of the stand for the dynamic impact on the course fork in the form of an angular operating speed of 500 rad/s was carried out around the vertical axis of the stand. Rigid pinching along the stand base was taken as the boundary conditions. Bearings, gearboxes, gear rims were approximated by a system of rod elements of identical rigidity. To determine the stiffness of these elements, an algorithm and a program were developed. The calculation of the stand of a three-layer structure, consisting of carrier layers of a five-layer composite material and a filler between them, perceiving shear stresses and preventing the bearing layers from approaching, was carried out. The influence of the arrangement of layers of a five-layer composite material on the stress-strain state of the stand was studied. The most favorable arrangement of layers of the five-layer compositional state for the bearing capacity of the stand was revealed. The methods considered in the work are applicable to robotic systems made of composite materials containing bearings, gear rims, gearboxes, motors.

5 Acknowledgements

This work was supported financially by the Russian Science under the Scientific Project № 22-29-20299 (the recipient is K.Z. Khayrnasov, https://rscf.ru/project/22-29-20299/).

References

1. Y. Tian, C. Chen, W. Duan, Intelligent robotic systems for structural health monitoring: Applications and future trends. Automation in Construction, **139** (2022) doi.org/10.1016/j.autcon.2022.104273
2. B. Tao, Y. Feng, Y. Wu, Accuracy of dental implant surgery using dynamic navigation and robotic systems: An in vitro study, Journal of Dentistry, **123** (2022) doi.org/10.1016/j.jdent.2022.104170 robotic
3. Y. Tian, C. Chen, W. Duan, Intelligent robotic systems for structural health monitoring: Applications and future trends, Automation in Construction, **139** (2022) doi.org/10.1016/j.autcon.2022.104273
4. X. Xu, Y. Chen, Y. Gong, Assignment of parcels to loading stations in robotic sorting systems, Transportation Research Part E: Logistics and Transportation Review, **164** (2022) doi.org/10.1016/j.tre.2022.102808
5. G. Boschetti, M. Faccio, R. Minto, 3D collision avoidance strategy and performance evaluation for human–robot collaborative systems, Computers & Industrial Engineering, **179** (2023) doi.org/10.1016/j.cie.2023.109225
6. B. Lindqvist, S. Karlsson, G. Nikolakopoulos, Multimodality : Integrated combined legged-aerial mobility for subterranean search-and-rescue, Robotics and Autonomous Systems, **154** (2022) doi.org/10.1016/j.robot.2022.104134
7. Yi Guo, R. G. Parker, Stiffness matrix calculation rolling bearings using a finite element/contact mechanics model, Mechanism and Machine Theory (2012) doi:10.1016/j.mechmachtheory.2011.12.006
8. I. Hoopert, J. Tribology, 136 (2014)
9. P. R. N. Childs, Rolling Element Bearings , Mechanical Design (2021)
10. P. Dewangan, A. Parey, M. Haddar, Dynamic characteristics of a wind turbine gearbox with amplitude modulation and gravity effect: Theoretical and experimental investigation, Mechanism and Machine Theory, **167** (2021)
11. L. Liu, L. Zhu, X. Gou, Modeling and analysis of load distribution ratio and meshing stiffness for orthogonal spur-face gear drive under point contact, Mechanism and Machine Theory, **184** (2023) doi.org/10.1016/j.mechmachtheory.2023.105312
12. H.-G. Kim, R. Wiebe, Numerical investigation of stress states in buckled laminated composite plates under dynamic loading, Composite Structures, **235** (2020) doi.org/10.1016/j.compstruct.2019.111743
13. A. Vaibhav, A. Phadnis, V. Silberschmidt, Composites Under Dynamic Loads at High Velocities Comprehensive Composite Materials, Composite Materials, **8** (2018)
14. A. Chao Correas, H. Ghasemnejad, Analytical development on impact behaviour of composite sandwich laminates by differentiated loading regimes, Aerospace Science and Technology, **126** (2022) doi.org/10.1016/j.ast.2022.107658 1270-9638/
15. E. J. Barbero. Finite Element Analysis of Composite Materials Using ANSYS (2013)
16. O. G. Latyshev, A. B. Veremeychik, E. A. Zhukov Application of composite materials in stands for dynamic loading, Moscow, Publishing house of MSTU N.E. Bauman (2011)
17. L. M. Gavva, V. V. Firsanov, Mechanics of Solids (Springer), **3** (2020)

18. O. V. Mitrofanov, Natural and Technical Sciences, **2(153)** (2021)
19. V. V. Vasiliev, E. V. Morozov, Advanced Mechanics of Composite Materials and Structures, Elsevier (2018)
20. A. Manes, A. Gilioli, C. Sbarufatti, M. Giglio, Experimental and numerical investigations of low velocity impact on sandwich panels, Compos., Struct. 99 (2013) doi.org/10.1016/j.compstruct.2012.11.031.
21. O. C. Zienkiewicz, R. L. Taylor, J. Z. Zhu, Finite element method: its basis and fundamental, Butterworth-Heinemann, Oxford (2013)
22. S. Moaveni, Finite Element Analysis Theory and Application with ANSYS, Pearson Education, London (2015)
23. I. Koutromanos, Applied Fundamentals of Finite Element Analysis Linear Finite Element Analysis, John Wiley & Sons, New York (2018)
24. K. J. Bathe, Finite element procedures, Pearson education Inc., New York (2006)
25. A. Noman, M. Shohel, S. Gupta, *Investigate the mechanical strength of laminated composite carbon fiber with different fiber orientations by numerically using finite element analysis*, Material, Proceedings (2023) doi.org/10.1016/j.matpr.2023.02.132
26. J.-P. Lin, X. Liu, G. Wang, Static and dynamic analysis of three-layered partial-interaction composite structures, Engineering Structures, 252 (2021) doi.org/10.1016/j.engstruct.2021.113581
27. B. Zhang, J. Ge, J. Liang, Failure prediction for fiber reinforced polymer composites based on virtual experimental tests, Journal of Materials Research and Technology, 24 (2023)
28. I. Daniel, Yield and failure criteria for composite materials under static and dynamic loading. Prog. Aero Sci, **81**, 18e25 (2016) doi.org/10.1016/j.paerosci.2015.11.003.
29. J. Gu, P. Chen, L. Su, K. Li, A theoretical and experimental assessment of 3D macroscopic failure criteria for predicting pure inter-fiber fracture of transversely isotropic UD composites. Compos. Struct., 259 (2021) doi.org/10.1016/ j.compstruct.2020.113466
30. Q. Sun, G. Zhou, Z. Meng, H. Guo, Z. Chen, H. Liu, H. Kang, S. Keten, X. Su, Failure criteria of unidirectional carbon fiber reinforced polymer composites informed by a computational micromechanics model. Compos Sci Technol., 172 (2019) doi.org/10.1016/ j.compscitech.2019.01.012.